A Dual Method for Computing Power Transfer Distribution Factors

Henrik Ronellenfitsch, Marc Timme, and Dirk Witthaut

Abstract—Power Transfer Distribution Factors (PTDFs) play a crucial role in power grid security analysis, planning, and redispatch. Fast calculation of the PTDFs is therefore of great importance. In this paper, we present a non-approximative dual method of computing PTDFs. It uses power flows along topological cycles of the network but still relies on simple matrix algebra. At the core, our method changes the size of the matrix that needs to be inverted to calculate the PTDFs from $N \times N$, where N is the number of buses, to $(L - N + 1) \times (L - N + 1)$, where L is the number of lines and $L - N + 1$ is the number of independent cycles (closed loops) in the network while remaining mathematically fully equivalent. For power grids containing a relatively small number of cycles, the method can offer a speedup of numerical calculations.

Index Terms—DC power flow, line outage distribution factor, power transfer distribution factor.

I. Introduction

THE supply of electric power is essential for the function of the economy as well as for our daily life. Because of their enabling function for other infrastructures such as traffic or health care, power systems are considered to be uniquely important [1]–[4]. The rise of renewable power sources puts new challenges to grid operation and security, as they are typically strongly fluctuating and often located far away from the load centers such that power must be transported over large distances [1], [5]–[7]. Thus efficient numerical methods are of great importance to analyze and improve the operation of power grids.

An important method to assess the security of a power grid and to detect impending overloads is given by the linear sensitivity

factors [8]. Power transfer distribution factors (PTDFs) describe how the real power flows change if power injection is shifted from one node to another. Correspondingly, line outage distribution factors (LODFs) describe the flow changes when one line fails. These elementary distribution factors can be generalized to reactive power flow [9] and multiple line outages [10]. PTDFs and LODFs are heavily used in the planning, monitoring and analysis of power systems [8], for instance for security analysis and contingency screening [11]–[13], island detection [14], the simulation of cascading failures [15], transmission congestion management [16], the estimation of available transfer capabilities [17], and re-dispatching in case of impending overloads [18], [19].

The numerical simulation of large interconnected power systems can be computationally demanding. A particularly demanding step in the calculation of PTDFs is the inversion of the nodal susceptance matrix whose size is given by the number of buses N in the grid. Computation times can be crucial when many different load configurations of the grid have to be considered or for real-time security analysis.

In this paper we propose a new approach to computing PTDFs in linear sensitivity analysis. It uses a decomposition of power flows into cycle flows. Suppose we inject some real power at node s and take it out at node r. We can satisfy real power balance by sending the power along an arbitrary path from s to r. Obviously, this does not yield the physical solution and must be corrected by flows over alternative paths from s to r. Our analysis offers a systematic way to obtain the physically correct solution by adding cycle flows which do not affect the power balance. This approach yields a novel method for calculating the PTDFs which can be more efficient than established alternatives. In particular, the size of the matrix which has to be inverted is given by the number of independent cycles in the network, which is often much smaller than N.

II. The DC Approximation and Linear Sensitivity Analysis

The operation of power grids is determined by the conservation of real and reactive power, also called Tellegen's theorem [8], [20]. The real power balance at one of the nodes $n = 1, \ldots, N$ reads

$$
P_n = g_{nn} V_n^2 - \sum_{k \neq n} \left(V_n V_k g_{nk} \cos(\theta_k - \theta_n) \right.
$$
$$
\left. + V_n V_k b_{nk} \sin(\theta_k - \theta_n) \right), \qquad (1)
$$

where P_n is the real power injection, i.e., the difference of generation and demand at the node n. The nodal voltage has magnitude V_n and the phase angle θ_n. The nodes are connected by transmission lines or transformers with conductance g_{nk} and susceptance b_{nk}. Within the dc approximation one neglects ohmic losses, $g_{\mathrm{nk}} = 0$, assumes that the voltage magnitude remains fixed and linearizes the sine function [8], [20]. In the simplest case one expands the sine around the 'empty' grid $\sin(\theta_k - \theta_n) \approx \theta_k - \theta_n$ and sets all voltages magnitudes to 1 p.u. The nodal voltage angles are then determined by the linear set of equations

$$\boldsymbol{B}\boldsymbol{\theta} = \boldsymbol{P} \qquad (2)$$

where $\boldsymbol{B} \in \mathbb{R}^{N \times N}$ is the nodal susceptance matrix with elements

$$B_{\mathrm{nk}} = \begin{cases} \sum_{j=1}^{N} b_{\mathrm{nj}} & \text{if} \quad k = n; \\ -b_{\mathrm{nk}} & \text{if} \quad k \neq n. \end{cases} \qquad (3)$$

The vectors $\boldsymbol{\theta} = (\theta_1, \dots, \theta_N)^t \in \mathbb{R}^N$ and $\boldsymbol{P} = (P_1, \dots, P_N)^t \in \mathbb{R}^N$ summarize the nodal voltage angles and the real power injections, respectively. Here and in the following the superscript 't' denotes the transpose of a vector or matrix. The real power flow from node k to n is then given by $F_{\mathrm{kn}} = b_{\mathrm{kn}}(\theta_k - \theta_n) = -B_{\mathrm{kn}}(\theta_k - \theta_n)$.

We now consider an increase of the real power injection at node s and a corresponding decrease at node r by the amount ΔP. The new vector of real power injections is given by

$$\boldsymbol{P}' = \boldsymbol{P} + \Delta P \, \boldsymbol{q}_{\mathrm{sr}}, \qquad (4)$$

where the components of $\boldsymbol{q}_{\mathrm{sr}} \in \mathbb{R}^N$ are $+1$ at position s, -1 at position r and zero otherwise. In the interest of reducing notational clutter, we omit the explicit dependence of $\boldsymbol{P}'$ on s and r. The nodal voltage angles then change by

$$\Delta\boldsymbol{\theta} = \Delta P \, \boldsymbol{X} \boldsymbol{q}_{\mathrm{sr}}, \qquad (5)$$

where $\boldsymbol{X}$ is the Moore–Penrose pseudo inverse of the nodal susceptance matrix,

$$\boldsymbol{X} = \boldsymbol{B}^{-1}. \qquad (6)$$

Again, we omit the explicit dependence on s and r. It is noted that $\boldsymbol{B}$ is a Laplacian matrix, which has one zero eigenvalue with eigenvector $(1, 1, \dots, 1)^t$ [21]. This eigenvector corresponds to a global shift of the voltage angles which has no physical significance. Finally, the real power flows change by $\Delta F_{\mathrm{ij}} = b_{\mathrm{ij}}(\Delta\theta_i - \Delta\theta_j)$ and the associated PTDFs are given by [8],

$$\begin{aligned} \mathrm{PTDF}_{(i,j),s,r} &:= \frac{\Delta F_{\mathrm{ij}}}{\Delta P} \\ &= b_{\mathrm{ij}}(X_{\mathrm{is}} - X_{\mathrm{ir}} - X_{\mathrm{js}} + X_{\mathrm{jr}}). \end{aligned} \qquad (7)$$

LODFs describe how the power flows change when a line (s, r) is lost. They are defined as [8]

$$\mathrm{LODF}_{(\mathrm{ij}),(\mathrm{sr})} = \frac{\Delta F_{\mathrm{ij}}}{F_{\mathrm{sr}}^{(0)}} \qquad (8)$$

where the superscript (0) denotes the flow before the outage.

The LODFs can be expressed by PTDFs in the following way. To consistently model the outage of line (s, r), one assumes that

the line is disconnected from the grid by circuit breakers and that some fictitious real power ΔP is injected at node s and taken out at node r. The entire flow over the line (s, r) after the opening thus equals the fictitious injections $F'_{\mathrm{sr}} = \Delta P$. Using PTDFs, we also know that

$$F'_{\mathrm{sr}} = F_{\mathrm{sr}}^{(0)} + \mathrm{PTDF}_{(s,r),s,r} \, \Delta P \qquad (9)$$

Substituting $F'_{\mathrm{sr}} = \Delta P$ and solving for ΔP yields

$$\Delta P = F'_{\mathrm{sr}} = \frac{F_{\mathrm{sr}}^{(0)}}{1 - \mathrm{PTDF}_{(s,r),s,r}} \qquad (10)$$

The change of real power flows of all other lines is given by $\Delta F_{\mathrm{ij}} = \mathrm{PTDF}_{(i,j),s,r} \Delta P$ such that we finally obtain

$$\mathrm{LODF}_{(\mathrm{ij}),(\mathrm{sr})} = \frac{\mathrm{PTDF}_{(i,j),s,r}}{1 - \mathrm{PTDF}_{(s,r),s,r}}. \qquad (11)$$

The accuracy of the dc approximation and correspondingly the PTDFs and LODFs can be increased if one linearizes around a solved AC power flow base case, i.e., one linearizes the equations (1) around one particular solution. This approach leads to so-called 'hot-start dc models' or 'incremental dc models' [22]–[24]. The governing equation of these advanced dc models is still given by (2), but $\boldsymbol{P}$ and $\boldsymbol{\theta}$ now describe the change of the power injections and phase angles with respect to the base case. The matrix $\boldsymbol{B}$ explicitly depends on the base case, such that a new matrix has to be inverted for every base case under consideration to compute the PTDFs and LODFs. If many such base cases need to be analyzed, any speedup of the computation can be extremely valuable.

III. FROM EDGE SPACE TO CYCLE SPACE

In this section, we review some basic linear algebraic methods from graph theory that we use in the rest of the paper. We mainly follow [25] and [21].

The connectivity structure of power transmission grids can be modeled as a graph. A graph $G = (V, E)$ consists of a set $V = \{v_1, \dots v_N\}$ of nodes (buses) and a set $E = \{e_1, \dots e_L\}$ of edges (transmission lines or branches), where each $e_\ell \in E$ connects two nodes, $e_\ell = \{v_{\ell_1}, v_{\ell_2}\}, v_{\ell_{1,2}} \in V$. Choosing an arbitrary but fixed orientation of the edges, the graph can be encoded in terms of the node-edge incidence matrix $\boldsymbol{I} \in \mathbb{R}^{N \times L}$ [21] with components

$$I_{n,\ell} = \begin{cases} 1 & \text{if node } n \text{ is the tail of edge } e_\ell, \\ -1 & \text{if node } n \text{ is the head of edge } e_\ell, \\ 0 & \text{otherwise.} \end{cases} \qquad (12)$$

The vector space $\mathcal{V} \simeq \mathbb{R}^N$ is called the *node space* of G and the vector space $\mathcal{E} \simeq \mathbb{R}^L$ is called the *oriented edge space* of G. $\mathcal{V}$ is spanned by the basis vectors $\boldsymbol{v}_i = (0, \dots, 0, 1, 0, \dots 0)^t \in \mathbb{R}^N$ with a 1 at the ith position and zeros everywhere else. Each basis vector $\boldsymbol{v}_i \in \mathcal{V}$ is associated with the node $v_i \in V$. Similarly, the edge vector space $\mathcal{E}$ is spanned by the basis vectors $\boldsymbol{e}_\ell = (0, \dots, 0, 1, 0, \dots 0)^t \in \mathbb{R}^L$, with one 1 at the ℓth position and is associated to the oriented edge $e_\ell \in E$.

The nullspace $\ker \boldsymbol{I}$ of the node-edge incidence matrix is called the *cycle space* $\mathcal{C}$ and its elements consist of all closed
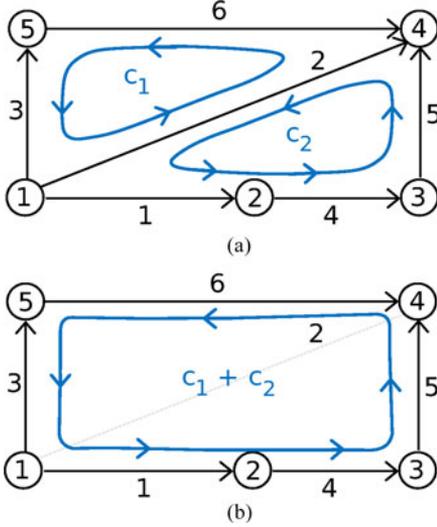
Fig. 1. Adding oriented cycles corresponds to the operation of symmetric difference. (a) A basis of the cycle space $\mathcal{C} \simeq \mathbb{R}^2$ is given by the vectors $\boldsymbol{c}_1 = (0, 1, -1, 0, 0, 0, -1)^t$ and $\boldsymbol{c}_2 = (1, -1, 0, 1, 1, 0)^t$. Note that $L = 6, N = 5$ such that $L - N + 1 = 2$. (b) A third cycle is obtained by forming the linear combination $\boldsymbol{c}_3 = \boldsymbol{c}_1 + \boldsymbol{c}_2 = (1, 0, -1, 1, 1, -1)$. Because the edges are oriented, this linear combination corresponds to the symmetric difference of edge sets.

oriented paths (cycles) of G. Each cycle path is represented by a vector $\boldsymbol{c} \in \mathbb{R}^L$ containing a $+1$ (if the edge oriented in the same way as the cycle) or a -1 (if the edge is oriented in the opposite way from the cycle) for each edge that is part of the cycle. It can be shown that $\mathcal{C} \simeq \mathbb{R}^{L-N+k} \subset \mathbb{R}^L$, where k is the number of connected components of G [25]. In the following, we will consider the case $k = 1$ without loss of generality because each connected component can be analyzed separately. Thus, there exists a basis of $L - N + 1$ cycles from which all other cycles can be obtained by (integer) linear combination. Forming a linear combination with coefficients in $\{-1, 0, 1\}$ such that edges contained in more than one cycle cancel is equivalent to the set-theoretic operation of symmetric difference [25] between the edge sets making up the cycles (see Fig. 1). The symmetric difference of two sets A and B is defined as the set $(A \cup B) \setminus (A \cap B)$. It contains all elements that are contained in either A or B but not in both.

One cycle basis for G is constructed as follows. Let $\mathcal{T}$ be a minimum spanning tree of G. We note that such a minimum spanning tree contains exactly $N - 1$ edges. For each edge $e \notin \mathcal{T}$, a cycle is defined by the set of e together with the path in $\mathcal{T}$ connecting the nodes of e. There are exactly $L - N + 1$ such cycles, one for each edge not in $\mathcal{T}$. They are linearly independent because each of them contains at least one edge not found in the others (e), thus they make up a basis of $\mathcal{C}$.

Given such a basis of cycles $\{c_1, \ldots, c_{L-N+1}\}$, we can now define the cycle-edge incidence matrix $\boldsymbol{C} \in \mathbb{R}^{L \times (L-N+1)}$ by

$$C_{\ell,c} = \begin{cases} 1 & \text{if edge } \ell \text{ is element of cycle } c, \\ -1 & \text{if reversed edge } \ell \text{ is element of cycle } c, \quad (13) \\ 0 & \text{otherwise.} \end{cases}$$

An explicit calculation shows that the matrix product

$$\boldsymbol{I}\boldsymbol{C} = \boldsymbol{0} \in \mathbb{R}^{N \times (L-N+1)}. \quad (14)$$

IV. DUAL METHOD

In this section, we introduce an alternative approach to network flows based on the dual representation of the network. This method can speed up computations considerably and also sheds some light on topological aspects of power flows. We note that the term duality here refers to the fact that the PTDFs can be calculated equivalently using voltage angles or cycle flows. However, in power grids with few cycles, there are much fewer cycle flows to compute than voltage angles, thus making the cycle flow method more economical. To start, we reformulate the dc model in a in a compact matrix notation.

Consider a grid with N nodes and L transmission lines or transformers. The real power injections $\boldsymbol{P}$ and the voltage angles $\boldsymbol{\theta}$ are associated with the nodes of the network, i.e., they are elements of $\mathbb{R}^N$. In contrast, power flows and susceptances are associated with lines, i.e., they are represented by elements of $\mathbb{R}^L$. To be precise, we label all transmission lines by $\ell = 1, \ldots, L$. We then have a mapping between ℓ and an ordered pair of nodes (i, j). The ordering is arbitrary but must kept fixed as we are dealing with directed quantities such as power flows. This mapping is encoded in the node-edge incidence matrix $\boldsymbol{I} \in \mathbb{R}^{N \times L}$. Let F_ℓ denote the real power flows on the line ℓ and define the vector $\boldsymbol{F} = (F_1, \ldots, F_L) \in \mathbb{R}^L$. The susceptances b_ℓ of the transmission lines are summarized in the branch susceptance matrix $\boldsymbol{B}_d = \text{diag}(b_1, \ldots, b_L) \in \mathbb{R}^{L \times L}$ and the branch reactance matrix $\boldsymbol{X}_d = \text{diag}(1/b_1, \ldots, 1/b_L) \in \mathbb{R}^{L \times L}$ The nodal susceptance matrix then reads $\boldsymbol{B} = \boldsymbol{I}\boldsymbol{B}_d\boldsymbol{I}^t$.

Within the dc approximation (2), the voltage angles and the flows are then written as

$$\boldsymbol{\theta} = (\boldsymbol{I}\boldsymbol{B}_d\boldsymbol{I}^t)^{-1}\boldsymbol{P},$$
$$\boldsymbol{F} = \boldsymbol{B}_d\,\boldsymbol{I}^t\boldsymbol{\theta}. \quad (15)$$

In practical applications it is common to define a PTDF matrix which summarizes the distribution factors for all lines $\ell \in \{1, \ldots, L\}$ and all nodes $r \in \{1 \ldots, N\}$, fixing the slack node s. For notational convenience we define the matrix $\boldsymbol{S} \in \mathbb{R}^{N \times N}$ generalizing the injection vectors $\boldsymbol{q}_{\text{sr}}$ used above,

$$S_{ij} = \begin{cases} -1 & \text{if } i = j \neq s, \\ +1 & \text{if } i = s, j \neq s, \quad (16) \\ 0 & \text{otherwise.} \end{cases}$$

The PTDF matrix for a given slack node s then reads

$$\mathbf{PTDF} = \boldsymbol{B}_d\boldsymbol{I}^t\,(\boldsymbol{I}\boldsymbol{B}_d\boldsymbol{I}^t)^{-1}\,\boldsymbol{S}. \quad (17)$$

For the calculation of the LODFs we do not fix a slack node s but consider the case where power ΔP is injected at one end of a line ℓ and withdrawn at the other end. This is described by the matrix

$$\mathbf{PTDF}' = \boldsymbol{B}_d\boldsymbol{I}^t\,(\boldsymbol{I}\boldsymbol{B}_d\boldsymbol{I}^t)^{-1}\,\boldsymbol{I} \quad (18)$$

such that the LODFs read

$$\mathbf{LODF}' = \mathbf{PTDF}'\,(\mathbb{1} - \text{diag}(\mathbf{PTDF}'))^{-1}, \quad (19)$$

where diag denotes the diagonal part of a matrix.

The standard approach to the calculation of PTDFs focuses on the nodes of the grid and the computationally most demanding step is the inversion of the nodal susceptance matrix $\boldsymbol{B} \in \mathbb{R}^{N \times N}$. As an alternative, we propose a method that works with the real power flows directly. Assume that additonal real power ΔP is injected at the slack node s and taken out at node r. To find the change of the power flows we proceed in two steps. First, we construct all vectors $\Delta \boldsymbol{F}$ which satisfy the real power balance: The sum of all flows incident to a node must equal the injected real power, $+\Delta P$ at node s, $-\Delta P$ at node r and zero otherwise, cf. equation (1). In vectorial form this condition can be written as

$$\Delta P \boldsymbol{q}_{\mathrm{rs}} \stackrel{!}{=} \boldsymbol{I} \Delta \boldsymbol{F} \tag{20}$$

Then we single out the vector which yields the correct voltage angles $\Delta \boldsymbol{\theta}$, see (5).

Any vector of flows $\Delta \boldsymbol{F}$ transporting the real power ΔP from node s to node r can be decomposed into two parts: a flow of magnitude ΔP on an arbitrary path from node s to node r plus an arbitrary amount of cycle flows which do not affect the power balance at any node. This decomposition is illustrated in Fig. 3(c) for a simple example network.

The set of paths from a fixed slack node s to all other nodes in the grid is referred to as a spanning tree in graph theory and can be calculated using efficient algorithms [25]. A spanning tree is generally not unique; an arbitrary one can be chosen for our purposes. It is most convenient to encode the paths by a matrix $\boldsymbol{T} \in \mathbb{R}^{L \times N}$ with the components

$$T_{\ell,r} = \begin{cases} 1 & \text{if line } \ell \text{ is element of path } s \to r, \\ -1 & \text{if reversed line } \ell \text{ is element of path } s \to r, \\ 0 & \text{otherwise.} \end{cases} \tag{21}$$

A power flow of magnitude ΔP from node s to r is then given by one vector $\Delta \boldsymbol{F} = \Delta P \boldsymbol{T}_{\cdot,r}$, where $\boldsymbol{T}_{\cdot,r}$ denotes the rth column of the matrix $\boldsymbol{T}$.

Furthermore, we need to characterize the cycle flows in the grid. We denote the strength of the cycle flows by f_c and define the vector $\boldsymbol{f} = (f_1 \ldots, f_{L-N+1}) \in \mathbb{R}^{L-N+1}$, where $L - N + 1$ is the number of independent cycles. The flow vector $\Delta \boldsymbol{F}$ is then written as the direct flow and an arbitrary linear combination of cycle flows as

$$\Delta \boldsymbol{F} = \Delta P \boldsymbol{T}_{\cdot,r} + \boldsymbol{C} \boldsymbol{f}, \tag{22}$$

where $\boldsymbol{C} \in \mathbb{R}^{L-N+1}$ is the cycle-edge incidence matrix (13). For any choice of $\boldsymbol{f}$, $\Delta \boldsymbol{F}$ satisfies the real power balance at each node because $\boldsymbol{I} \boldsymbol{C} = \boldsymbol{0}$.

In a second step, we determine the correct physical flow vector $\Delta \boldsymbol{F}$. This amounts to calculating the cycle flow strengths $\boldsymbol{f}$ such that all voltage angles in the grid are unique. A necessary and sufficient condition is that the sum of all angle differences along any closed cycle equals zero,

$$\sum_{(\mathrm{ij}) \in \text{cycle } c} (\Delta \theta_i - \Delta \theta_j) \stackrel{!}{=} 0. \tag{23}$$

As the cycles form a vector space it is sufficient to check this condition for the $L - N + 1$ basis cycles. Using $\Delta F_{\mathrm{ij}} =$

Construct the cycle-edge incidence matrix $\boldsymbol{C}$, the spanning tree matrix $\boldsymbol{T}$, and the branch reactance matrix $\boldsymbol{X}_d$.

↓

Form the matrices $\boldsymbol{X}_T = \boldsymbol{C}^t \boldsymbol{X}_d \boldsymbol{T}$, and $\boldsymbol{X}_C = \boldsymbol{C}^t \boldsymbol{X}_d \boldsymbol{C}$.

↓

Solve the linear system $\boldsymbol{X}_C \boldsymbol{Y} = \boldsymbol{X}_T$.

↓

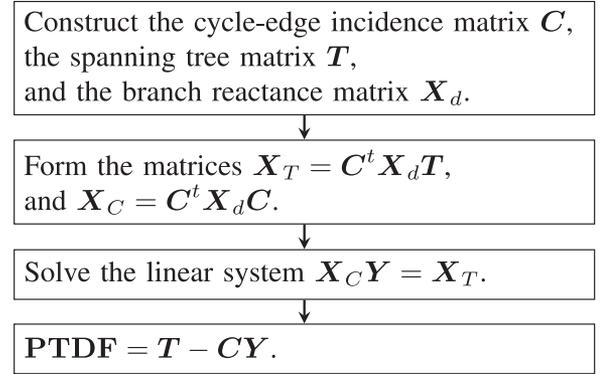$\mathbf{PTDF} = \boldsymbol{T} - \boldsymbol{C} \boldsymbol{Y}$.

Fig. 2. Flow chart describing how to use the dual method to compute the PTDF matrix from equation (28).

$b_{\mathrm{ij}}(\Delta \theta_i - \Delta \theta_j)$, the condition reads

$$\sum_{(\mathrm{ij}) \in \text{cycle } c} \Delta F_{\mathrm{ij}}/b_{\mathrm{ij}} \stackrel{!}{=} 0 \tag{24}$$

for all basis cycles $c \in \{1, \ldots, L - N + 1\}$. This set of equations can be recast into matrix form,

$$\boldsymbol{C}^t \boldsymbol{X}_d \Delta \boldsymbol{F} = \boldsymbol{0}. \tag{25}$$

Inserting the decomposition (22) we obtain

$$\boldsymbol{C}^t \boldsymbol{X}_d \boldsymbol{C} \boldsymbol{f} + \Delta P \boldsymbol{C}^t \boldsymbol{X}_d \boldsymbol{T}_{\cdot,r} = \boldsymbol{0}, \tag{26}$$

which can be solved for the cycle flows $\boldsymbol{f}$. The formal solution is

$$\boldsymbol{f} = -\Delta P (\boldsymbol{C}^t \boldsymbol{B}_d^{-1} \boldsymbol{C})^{-1} \boldsymbol{C}^t \boldsymbol{B}_d^{-1} \boldsymbol{T}_{\cdot,r}. \tag{27}$$

The changes of the real power flows are given by equation (22). The PTDF matrix summarizing the distribution factors for all nodes r and a fixed slack bus s is then calculated by inserting equation (27) into equation (22) and subsequently using the definition (7). The result is

$$\mathbf{PTDF} = \left[\mathbb{1} - \boldsymbol{C}(\boldsymbol{C}^t \boldsymbol{X}_d \boldsymbol{C})^{-1} \boldsymbol{C}^t \boldsymbol{X}_d \right] \boldsymbol{T}. \tag{28}$$

An efficient way of using this formula is shown in the flow chart Fig. 2.

For the calculation of the LODFs we do not need to calculate the matrix $\boldsymbol{T}$, as only injections at the terminal end of the lines $\ell = 1, \ldots, L$ are considered. The LODF matrix is given by equation (19) with

$$\mathbf{PTDF}' = \left[\mathbb{1} - \boldsymbol{C}(\boldsymbol{C}^t \boldsymbol{X}_d \boldsymbol{C})^{-1} \boldsymbol{C}^t \boldsymbol{X}_d \right], \tag{29}$$

where the derivation proceeds analogously to that of equation (28).

We stress that equation (28) is not an approximation to the conventional equation (17), it is an alternative but mathematically fully equivalent way of computing the PTDFs. There are no approximations involved in the transformation to the dual description. The applicability of linear distribution factors itself is discussed in [22]–[24], [26].
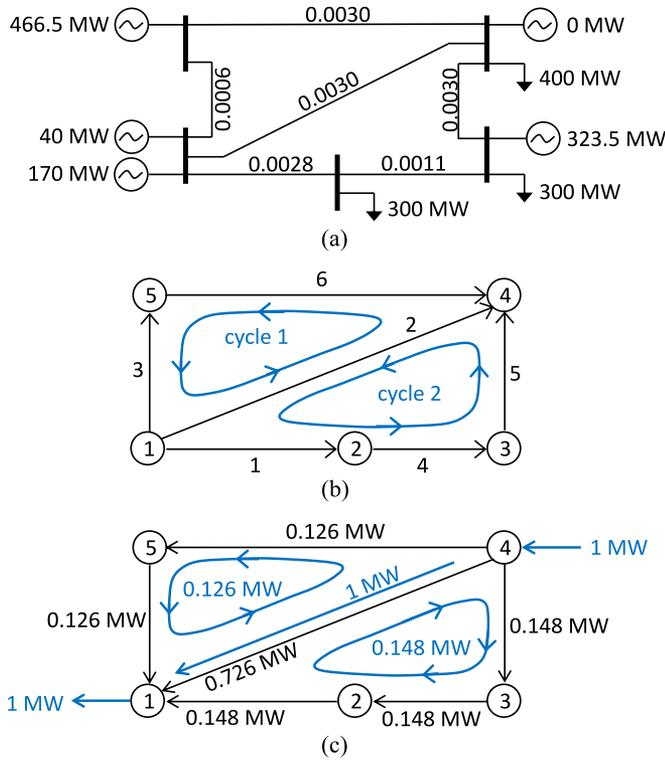
Fig. 3. Physical and cycle flows in a five-bus example network (a) Circuit diagram of the five-bus example network [27]. The reactances of each line are given in p.u. (b) Topology of the network. Labels of nodes, lines and cycles as used in the text. (c) Calculation of PTDFs. Black numbers give the physical power flow $\Delta \boldsymbol{F}$ when 1 MW is injected at node 4 and withdrawn at node 1. The flows ΔF can be decomposed into a 1 MW-flow from node 4 to node 1 on the direct path plus two cycle flows shown by blue arrows.

V. EXAMPLE

As an instructive example we consider the five-bus test grid from MATPOWER [27] with $N = 5$ and $L = 6$. The circuit diagram as well as the topology of the grid are illustrated in Fig. 3. The node-edge incidence matrix is given by

$$\boldsymbol{I} = \begin{pmatrix} +1 & +1 & +1 & 0 & 0 & 0 \\ -1 & 0 & 0 & +1 & 0 & 0 \\ 0 & 0 & 0 & -1 & +1 & 0 \\ 0 & -1 & 0 & 0 & -1 & -1 \\ 0 & 0 & -1 & 0 & 0 & +1 \end{pmatrix}. \quad (30)$$

The grid contains 2 independent cycles, which are chosen as
   cycle 1: line 2, reverse line 6, reverse line 3.
   cycle 2: line 1, line 4, line 5, reverse line 2
   The cycle-edge incidence matrix thus reads

$$\boldsymbol{C}^t = \begin{pmatrix} 0 & +1 & -1 & 0 & 0 & -1 \\ +1 & -1 & 0 & +1 & +1 & 0 \end{pmatrix}. \quad (31)$$

Fig. 3(c) shows the physical real power flows as well as the cycle decomposition (22) for $s = 4$ and $r = 1$. There is a direct flow of magnitude $\Delta P = 1\,\mathrm{MW}$ from node 4 to node 1. Additional cycle flows along the two independent cycles do not affect the power balance. The physical flows are recovered when the strength of the cycle flows is given by $f_1 = 0.126\,\mathrm{MW}$ and $f_2 = -0.148\,\mathrm{MW}$.

The example shows how the new method can potentially speed-up the computation of PTDFs. The conventional approach focuses on the $N = 5$ nodes of the grid and calculates how the voltage angles change. But these $N = 5$ variables are not independent but related topologically through the condition (23). In the new approach only 2 independent variables, the cycle flow strengths, must be calculated. The changes in power flow then follow directly from (22) and the PTDFs from (28).

VI. IMPLEMENTATION AND COMPUTATIONAL PERFORMANCE

The computationally most demanding part in the calculation of PTDFs is the inversion of a large matrix. In the conventional approach defined by equation (17), the $N \times N$-matrix $\boldsymbol{B} = \boldsymbol{I}\boldsymbol{B}_d\boldsymbol{I}^t$ has to be inverted. The dual method defined by equation (28) requires the inversion of a $(L - N + 1) \times (L - N + 1)$-matrix $\boldsymbol{C}^t\boldsymbol{X}_d\boldsymbol{C}$ instead. In real-world power grids, the number of cycles $L - N + 1$ is often much smaller than N. Hence a much smaller matrix has to be inverted which can lead to a significant speed-up of numerical calculations.

In practical applications, the formula (17) for the conventional computation of PTDFs is usually slightly modified. As noted before, the nodal susceptance matrix $\boldsymbol{B}$ has one zero eigenvalue associated with a global shift of the voltage angles. One generally fixes the voltage angle at the slack node s at a value of zero and excludes this node from the calculation. Equation (17) then reads

$$\mathbf{PTDF}_{\mathrm{red}} = \boldsymbol{B}_{f,\mathrm{red}}\,\boldsymbol{B}_{\mathrm{red}}^{-1}, \quad (32)$$

where $\boldsymbol{B}_f = \boldsymbol{B}_d\boldsymbol{I}^t$ and the subscript 'red' indicates that slack bus is excluded, i.e., the sth row and column is deleted in $\boldsymbol{B}$ and the sth column for all other matrices. Furthermore, one does not have to compute the full inverse of the matrices but can solve a system of linear equations instead. For instance, one can solve

$$\mathbf{PTDF}_{\mathrm{red}}\boldsymbol{B}_{\mathrm{red}} = \boldsymbol{B}_{f,\mathrm{red}}. \quad (33)$$

for $\boldsymbol{B}_{\mathrm{red}}$ instead of computing the inverse in equation (32). This approach is implemented for instance in the popular software package MATPOWER 5.1 [27].

The dual method yields the formula (28) for the computation of the PTDF matrix. Again one can omit the full matrix inversion and solve a linear system of equations instead. Then computation is then done in two steps

$$\text{Solve} \quad (\boldsymbol{C}^t\boldsymbol{X}_d\boldsymbol{C})\,\mathbf{TEMP} = (\boldsymbol{C}^t\boldsymbol{X}_d\boldsymbol{T})$$
$$\text{Compute} \quad \mathbf{PTDF} = \boldsymbol{T} - \boldsymbol{C}\,\mathbf{TEMP}. \quad (34)$$

If one is only interested in calculating LODFs by means of equations (19) and (29), a further speedup is possible by defining $\tilde{\boldsymbol{C}}^t = \boldsymbol{C}^t\sqrt{\boldsymbol{X}_d} = \boldsymbol{Q}\boldsymbol{R}$ using a QR decomposition. Then,

$$\mathbf{PTDF}' = \left[\mathbb{1} - \sqrt{\boldsymbol{B}_d}\boldsymbol{Q}\boldsymbol{Q}^t\sqrt{\boldsymbol{X}_d}\right], \quad (35)$$

completely eliminating the need for inverting any matrices.

A. Sparse Numerics

We test how the dual method presented in this paper can speed up actual computations using several test cases. We compare the

```
tic;
PTDF1 = zeros(L,N);
Bf = Bd * I';
Bbus = I * Bf;
PTDF1(:,an) = full(Bf(:,an)/Bbus(an,an));
toc

tic;
Xf = C' * Xd;
Xc = Xf * C;
Xt = Xf * T;
PTDF2 =  T - C * full(Xc \ Xt);
toc
```

Fig. 4. MATLAB code to compare the runtime of the conventional algorithm and the dual method. All variable names are same as those used in the text with the exception of an, which indexes all nodes except for the slack.

conventional method using Eq. (32) to the dual method given by Eq. (34). The runtimes of all methods are evaluated using the MATLAB script listed in Fig. 4. In addition, we evaluate the runtime for the solution of the linear set of equations alone, i.e., execution of the commands Bf(:,an)/Bbus(an,an) and Xc \Xt, respectively. The variable an is a vector indexing all nodes except for the slack node. All other variables are the same as before.

Because all input matrices involved exhibit a sparse structure (i.e., they contain many identically zero entries), it is sensible to test computational performance using specialized sparse numerics. To this end, we converted all input matrices appearing in the code of Fig. 4 into the sparse format used by MATLAB using the sparse command. Internally, MATLAB then employs the high-performance supernodal sparse Cholesky decomposition solver CHOLMOD 1.7.0 for the solution of the linear system of equations. The resulting PTDF matrix is full (i.e., it usually contains no zeros), such that we converted the results back to a full matrix using the command full. For the dual method, care has to be taken about where to do the conversion (see the code example in Fig. 4).

The results are shown in Table I and Fig. 5 for various test grids from [27]–[31]. For the sake of simplicity we have merged all parallel transmission lines, such that the graph contains no loops. Tests were carried out on a workstation with an Intel Xeon E5-2637v2 processor at 3.5 Ghz and 256 GB RAM using Windows 8.1Pro, MATLAB version R2015a and MATPOWER version 5.1. All results were averaged over 100 runs and the standard deviation is given.

We find that the dual method (34) significantly speeds up the computation for all test grids under considerations. The dual method is faster by a factor of up to 4.43 for transmission grids and up to 6.63 for distribution grids. The speed-up is even more pronounced if we consider the solution of the linear system only, ranging up to 12.08 for transmission grids and up to 75.03 for distribution grids. However, the dual methods requires additional matrix multiplications to construct the PTDFs, which reduces the total speed-up.

B. Dense Numerics

Traditional dense numerical performance is dominated by the dimensionality of the problem, which is given by the number of nodes N for the conventional method and the number of cycles $L - N + 1$ for the dual method. Hence, the ratio of the runtimes (the speedup) is essentially determined by the ratio $(L - N + 1)/N$. The speed-up obtained using the dual method is even larger than in the case of sparse numerics and reaches up to a factor of 5.06 for the transmission test grids and 19.89 for the distribution test grids studied here. Numerically, we find that the total speedup scales as a power law with the ratio of the number of cycles and the number of nodes $(L - N + 1)/N$ with an exponent $\gamma = 0.616$ (Fig. 6).

VII. POTENTIAL APPLICATIONS

A. Speeding Up Calculations

The dual method can significantly speed up the calculation of PTDFs depending on the network topology as shown in the previous section. Thus it can be useful for time-critical applications where PTDFs must be calculated repeatedly—for instance in 'hot-start dc models' or 'incremental dc models'. In these cases the matrix $\boldsymbol{B}$ is different for all base cases under consideration and the distribution factors have to be calculated separately for all cases (see [24] and references therein). For instance, in the flow-based approach to capacity allocation and congestion management in Europe, PTDFs must be calculated for each timeframe [32].

There are two main reasons making the dual method particularly suitable for this type of applications: First, the speedup can be significant but the absolute computation times are such that the conventional method is also feasible when the computation time is not critical. Second, the application of the dual method makes use of the spanning tree $\boldsymbol{T}$ and the cycle incidence matrix $\boldsymbol{C}$, the calculation of which also requires some computational resources. However, both $\boldsymbol{C}$ and $\boldsymbol{T}$ depend only on the network topology, but not on the actual values of B_{nk}. They are identical for all base cases such that they can be calculated once during initialization and stored for further use. Even more, they can be updated easily when a new bus or a transmission line is connected to the grid [33].

The speed-up is even more pronounced for distribution grids, which are ultra-sparse by construction. The use of PTDFs is less common in distribution grids, but has recently gained some interest in the control of grid congestion due to electric vehicle charging [34], [35].

B. Changes of the Grid Topology

In addition to purely numerical benefits, the dual formulation can be used to derive analytical results on how power flows in complex grid topologies. For example, it shows in an intuitive way how the flows are affected by changes of the grid topology. To demonstrate this we consider the closing of a tie-switch in a distribution grid. Assuming that the grid was tree-like in its original configuration, the closing induces a single unique cycle c and the cycle incidence matrix $\boldsymbol{C}$ reduces to a vector in $\mathbb{R}^L$.

Test Grid		Grid Size				CPU time in seconds		speedup
name	source	nodes N	lines L	cycles $L - N + 1$	cycles/nodes $\frac{L-N+1}{N}$	Conventional method Eq. (32)	Dual method Eq. (34)	$t_{(32)}/t_{(34)}$
Transmission grids:								
case300	[27]	300	409	110	0.37	0.0038 ± 0.0006	0.0020 ± 0.0005	1.90
case1354pegase	[28]	1354	1710	357	0.26	0.131 ± 0.006	0.038 ± 0.001	3.46
GBnetwork	[29]	2224	2804	581	0.26	0.38 ± 0.00	0.09 ± 0.00	4.43
case2383wp	[27]	2383	2886	504	0.21	0.45 ± 0.01	0.12 ± 0.00	3.72
case2736sp	[27]	2736	3495	760	0.28	0.63 ± 0.02	0.30 ± 0.02	2.06
case2746wp	[27]	2746	3505	760	0.28	0.646 ± 0.031	0.307 ± 0.031	2.11
case2869pegase	[28]	2869	3968	1100	0.38	0.709 ± 0.052	0.224 ± 0.002	3.16
case3012wp	[27]	3012	3566	555	0.18	0.696 ± 0.052	0.173 ± 0.014	4.04
case3120sp	[27]	3120	3684	565	0.18	0.735 ± 0.045	0.184 ± 0.020	3.99
westernus	[30]	4941	6594	1654	0.33	1.906 ± 0.079	0.669 ± 0.054	2.85
case9241pegase	[28]	9241	14207	4967	0.54	9.49 ± 0.97	7.61 ± 0.46	1.25
Distribution grids:								
bus_873_7	[31]	880	900	21	0.02	0.043 ± 0.000	0.007 ± 0.001	6.43
bus_10476_84	[31]	8489	8673	185	0.02	4.49 ± 0.43	0.68 ± 0.21	6.63

The PTDFs change as

$$\Delta\mathbf{PTDF} = -C(C^T X_d C)^{-1} C^T X_d T, \qquad (36)$$

which allows for a very simple interpretation. Consider the rth row of the PTDF matrix and assume that the root of the tree has been chosen as slack. Then we have

$$\Delta\mathbf{PTDF}_{\cdot,r} = -C \frac{\sum_{\ell \in \text{cycle } c \text{ and } \ell \in \text{path } s \to r} x_\ell}{\sum_{\ell \in \text{cycle } c} x_\ell}. \qquad (37)$$

This formulation shows two main aspects of flow rerouting due to the closing of the switch: First the PTDF matrix changes only for the lines which are part of the induced cycle. Second, the strength of the change is given by the ratio of two sums of line reactances: In the denominator we sum over all lines which are part of the cycle c and in the numerator we sum only over which are part of the cycle c *and* the direct path from the slack node s to node r. Loosely speaking, this ratio measures the overlap of the induced cycle and the direct path from s to r. This and similar results can also be obtained in a different way, but are immediately obvious in the dual formulation.

C. Quantifying Unscheduled Flows

Unscheduled power flows or loop flows refer to the fact that power can flow through several paths in a meshed grid, and thus lead to different flows than scheduled during trading. These flows significantly contribute to limits for limit cross border trading, e.g., in the interconnected European grid, and have played an important role in events like the 2003 North American blackout [36]–[38]. We here discuss the quantification of unscheduled flows on a nodal level. Unscheduled flows between different loop flows zones can be treated in the same manor using zonal PTDFs and effective line parameters [39], [40].

Suppose a generator at node s sells power P to a consumer at node r and let $\pi \in \mathbb{R}^L$ be a vector which encodes the scheduled path for the power flow. In the simplest case there is a direct connection between nodes s and r via the transmission line ℓ.
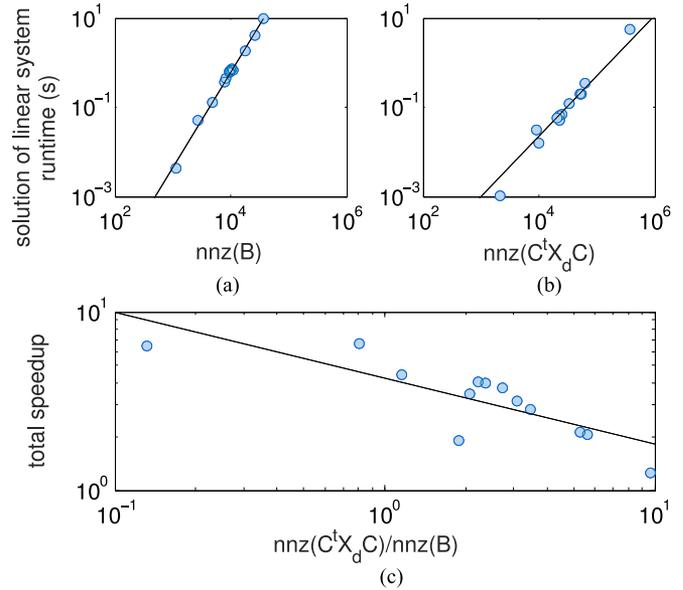

Fig. 5. Depending on network topology, the dual method can significantly speed up the calculation of the PTDFs. (a, b) The runtime of the linear inversion step using the MATLAB Cholesky decomposition solver scales with the number of non-zero elements ('nnz') of the matrices B and the matrix $C^t X_d C$, respectively. However, the scaling exponents and the prefactors are vastly different, such that the dual method is faster. (c) The total speed-up is given by the ratio of the runtimes of the conventional node-based method with fixed slack and the dual method including all matrix multiplications. The total speed-up lies between 1.25 and 6.63 for the test grids under consideration. The runtimes have been evaluated using the code listed in Fig. 4 and are listed in Table I. The black lines are power-law fits to the data.

Then π is a unit vector which is one at position ℓ and zero otherwise. Formula (28) now directly yields the actual, scheduled and unscheduled flows induced by this transaction:

$$F_{\text{actual}} = \underbrace{P\pi}_{=:F_{\text{scheduled}}} \underbrace{-PC(C^T X_d C)^{-1} C^T X_d \pi}_{=:F_{\text{unscheduled}}}. \qquad (38)$$
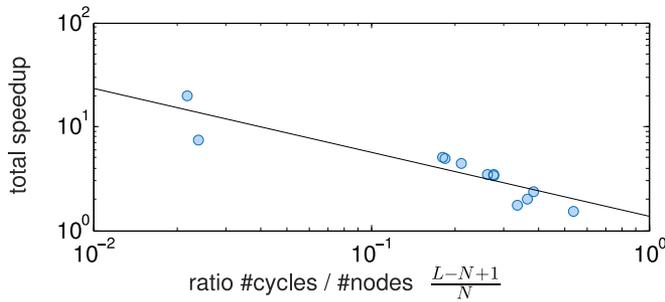
Fig. 6. Total speed-up of the dual method using dense numerics using the same test grids as in Fig. 5 as a function of the ratio of the numbers of cycles $L - N + 1$ and the number of nodes N. The black line is a power law fit $\alpha \times [(L - N + 1)/N]^{-\gamma}$ to the data, which yields the parameters $\alpha = 1.355$ and $\gamma = 0.616$.

VIII. CONCLUSION

PTDFs and LODFs are important tools enabling the efficient planning of power grid operations in contingency cases. Especially for very large networks, computational efficiency can be crucial. We presented a novel method of calculating the PDTFs based on cycle flows, eliminating redundant degrees of freedom present in the conventional approach. The main step of the computation is the solution of a large linear system of equations, whose dimensionality is reduced from the number of nodes N to the number of fundamental cycles $L - N + 1$, L being the number of branches. This can result in a significant improvement of the computation time for grids where the number of cycles $L - N + 1$ is significantly smaller than the number of nodes N. In addition, the cycle flow description provides a conceptual advantage, dealing with power flows directly without recourse to voltage angles. We finally note that mathematically equivalent models of flow are used to describe hydraulic networks [41] or vascular networks of plants [42].

REFERENCES

[1] S. M. Amin and B. F. Wollenberg, "Toward a smart grid: Power delivery for the 21st century," *IEEE Power Energy Mag.*, vol. 3, no. 5, pp. 34–41, Sep./Oct. 2005.

[2] P. Pourbeik, P. Kundur, and C. Taylor, "The anatomy of a power grid blackout—Root causes and dynamics of recent major blackouts," *IEEE Power Energy Mag.*, vol. 4, no. 5, pp. 22–29, Sep./Oct. 2006.

[3] W. Kröger, "Critical infrastructures at risk: A need for a new conceptual approach and extended analytical tools," *Rel. Eng. Syst. Safety*, vol. 93, no. 12, pp. 1781–1787, 2008.

[4] E. van der Vleuten and V. Lagendijk, "Transnational infrastructure vulnerability: The historical shaping of the 2006 European blackout," *Energy Policy*, vol. 38, no. 4, pp. 2042–2052, 2010.

[5] D. Heide, L. von Bremen, M. Greiner, C. Hoffmann, M. Speckmann, and S. Bofinger, "Seasonal optimal mix of wind and solar power in a future, highly renewable Europe," *Renew. Energy*, vol. 35, no. 11, pp. 2483–2489, 2010.

[6] M. Rohden, A. Sorge, M. Timme, and D. Witthaut, "Self-organized synchronization in decentralized power grids," *Phys. Rev. Lett.*, vol. 109, no. 6, p. 064101, 2012.

[7] T. Pesch, H.-J. Allelein, and J.-F. Hake, "Impacts of the transformation of the german energy system on the transmission grid," *Eur. Phys. J. Special Topics*, vol. 223, no. 12, pp. 2561–2575, 2014.

[8] A. J. Wood, B. F. Wollenberg, and G. B. Sheblé, *Power Generation, Operation and Control*. New York, NY, USA: Wiley, 2014.

[9] C.-Y. Lee and N. Chen, "Distribution factors of reactive power flow in transmission line and transformer outage studies," *IEEE Trans. Power Syst.*, vol. 7, no. 1, pp. 194–200, Feb. 1992.

[10] T. Güler, G. Gross, and M. Liu, "Generalized line outage distribution factors," *IEEE Trans. Power Syst.*, vol. 22, no. 2, pp. 879–881, May 2007.

[11] P. W. Sauer, "On the formulation of power distribution factors for linear load flow methods," *IEEE Trans. Power App. Syst.*, vol. PAS-100, no. 2, pp. 764–770, Feb. 1981.

[12] W. Y. Ng, "Generalized generation distribution factors for power system security evaluations," *IEEE Trans. Power App. Syst.*, vol. PAS-100, no. 3, pp. 1001–1005, Mar. 1981.

[13] B. Stott, O. Alsac, and A. J. Monticelli, "Security analysis and optimization," *Proc. IEEE*, vol. 75, no. 12, pp. 1623–1644, Dec. 1987.

[14] T. Guler and G. Gross, "Detection of island formation and identification of causal factors under multiple line outages," *IEEE Trans. Power Syst.*, vol. 22, no. 2, pp. 505–513, May 2007.

[15] I. Dobson, J. Chen, J. Thorp, B. Carreras, and D. Newman, "Examining criticality of blackouts in power system models with cascading events," in *Proc. 35th Annu. Hawaii Int. Conf. Syst. Sci.*, 2002, pp.–10.

[16] H. Singh, S. Hao, and A. Papalexopoulos, "Transmission congestion management in competitive electricity markets," *IEEE Trans. Power Syst.*, vol. 13, no. 2, pp. 672–680, May 1998.

[17] M. Gravener and C. Nwankpa, "Available transfer capability and first order sensitivity," *IEEE Trans. Power Syst.*, vol. 14, no. 2, pp. 512–518, May 1999.

[18] B. Stott, J. Marinho, and O. Alsac, "Review of linear programming applied to power system rescheduling," in *Proc. IEEE Conf. Power Ind. Comput. Appl. Conf.*, 1979, pp. 142–154.

[19] B. Marinescu, J. Coulondre, P. Tsamasphyrou, and J.-Y. Bourmaud, "Improving TSO's coordination for cross-border redispatch: A discussion of possible approaches in the European context," in *Proc. CIGRE/IEEE PES Int. Symp.*, 2005, pp. 378–385.

[20] J. J. Grainger and W. D. Stevenson Jr., *Power System Analysis*. New York, NY, USA: McGraw-Hill, 1994.

[21] M. E. J. Newman, *Networks—An Introduction*. Oxford, U.K.: Oxford Univ. Press, 2010.

[22] R. Baldick, "Variation of distribution factors with loading," *IEEE Trans. Power Syst.*, vol. 18, no. 4, pp. 1316–1323, Nov. 2003.

[23] R. Baldick, K. Dixit, and T. Oberbye, "Empirical analysis of the variation of distribution factors with loading," in *Proc. IEEE Power Eng. Soc. General Meeting*, 2005, pp. 221–229.

[24] B. Stott, J. Jardim, and O. Alsac, "DC power flow revisited," *IEEE Trans. Power Syst.*, vol. 24, no. 3, pp. 1290–1300, Aug. 2009.

[25] R. Diestel, *Graph Theory*. New York, NY, USA: Springer, 2010.

[26] D. Van Hertem, J. Verboomen, K. Purchala, R. Belmans, and W. Kling, "Usefulness of DC power flow for active power flow analysis with flow controlling devices," in *Proc. 8th IEEE Int. Conf. AC DC Power Transm.*, 2006, pp. 58–62.

[27] R. D. Zimmerman, C. E. Murillo-Sanchez, and R. J. Thomas, "Matpower: Steady-state operations, planning and analysis tools for power systems research and education," *IEEE Trans. Power Syst.*, vol. 26, no. 1, pp. 12–19, Feb. 2011.

[28] S. Fliscounakis, P. Panciatici, F. Capitanescu, and L. Wehenkel, "Contingency ranking with respect to overloads in very large power systems taking into account uncertainty, preventive and corrective actions," *IEEE Trans. Power Syst.*, vol. 28, no. 4, pp. 4909–4917, Nov. 2013.

[29] W. A. Bukhsh and K. McKinnon, Network data of real transmission networks, 2013. [Online]. Available: http://www.maths.ed.ac.uk/optenergy/NetworkData/

[30] D. J. Watts and S. H. Strogatz, "Collective dynamics of small-world networks," *Nature*, vol. 393, pp. 440–442, 1998.

[31] R. Kavasseri and C. Ababei, *Reds: Repository of distribution systems*. [Online]. Available: http://www.dejazzer.com/reds.html, accessed May 18, 2016. We consider the case where all tie-switches are closed. For the grid bus_10476_84, we consider only the largest connected component.

[32] *European Commission, Commission Regulation 2015/1222 establishing a guideline on capacity allocation and congestion management, 24 July 2015*. [Online]. Available: http://eur-lex.europa.eu/legal-content/EN/TXT/?uri=CELEX%3A32015R1222

[33] F. Chin and D. Houck, "Algorithms for updating minimal spanning trees," *J. Comput. Syst. Sci.*, vol. 16, no. 3, pp. 333–344, 1978.

[34] N. O'Connell, Q. Wu, J. Østergaard, A. H. Nielsen, S. T. Cha, and Y. Ding, "Day-ahead tariffs for the alleviation of distribution grid congestion from electric vehicles," *Elect. Power Syst. Res.*, vol. 92, pp. 106 –114, 2012.

[35] R. Li, Q. Wu, and S. S. Oren, "Distribution locational marginal pricing for optimal electric vehicle charging management," *IEEE Trans. Power Syst.*, vol. 29, no. 1, pp. 203–211, Jan. 2014.

[36] J. Bower, *Seeking the single European electricity market: evidence from an empirical analysis of wholesale market prices, Oxford Institute for Energy Studies, Tech. Rep. 286084*, 2002. [Online]. Available: https://www.oxfordenergy.org/publications/seeking-the-single-european-electricity-market-evidence-from-an-empirical-analysis-of-wholesale-market-prices/

[37] S. Suryanarayanan, "Techniques for accommodating unscheduled flows in electricity networks and markets," in *Proc. IEEE Power & Energy Soc. General Meeting-Convers. Del. Elect. Energy 21st Century*, 2008, pp. 1–6.

[38] A. Marinakis, M. Glavic, and T. V. Cutsem, "Minimal reduction of unscheduled flows for security restoration: Application to phase shifter control," *IEEE Trans. Power Syst.*, vol. 25, no. 1, pp. 506–515, Feb. 2010.

[39] K. Purchala, E. Haesen, L. Meeus, and R. Belmans, "Zonal network model of european interconnected electricity network," in *Proc. Int. Symp. CIGRE/IEEE PES*, 2005, pp. 362–369.

[40] B. Tranberg, A. B. Thomsen, R. A. Rodriguez, G. B. Andresen, M. Schäfer, and M. Greiner, "Power flow tracing in a simplified highly renewable european electricity network," *New J. Phys.*, vol. 17, no. 10, 2015, Art. no. 105002.

[41] N. Hwang and R. Houghtalen, *Fundamentals of Hydraulic Engineering Systems*. Upper Saddle River, NJ, USA: Prentice-Hall, 1996.

[42] E. Katifori, G. J. Szöllősi, and M. O. Magnasco, "Damage and fluctuations induce loops in optimal transport networks," *Phys. Rev. Lett.*, vol. 104, Jan. 2010, Art. no. 048704.

Marc Timme studied physics and applied mathematics at the Universities of Würzburg (Germany), Stony Brook (New York, USA) and Göttingen (Germany). He holds an M.A. in Physics from Stony Brook and a Doctorate in Theoretical Physics (Göttingen). After postdoctoral and visiting stays at Cornell University (New York, USA) and the National Research Center of Italy (Sesto Fiorentino) he is heading the Max Planck Research Group on Network Dynamics at the Max Planck Institute for Dynamics and Self-Organization. He is Adjunct Professor at the University of Göttingen.

Henrik Ronellenfitsch received the B.Sc. and M.Sc. degrees in physics from ETH Zürich, Switzerland, in 2010 and 2012, respectively. He received the Ph.D. degree from the Max Planck Institute for Dynamics and Self-Organization in Göttingen, Germany, in 2016 working on problems involving flow and transport networks as applied to biological and human-made systems and now works as a Postdoctoral Researcher at the Department of Physics and Astronomy, University of Pennsylvania.

Dirk Witthaut received the Diploma (M.Sc.) and Ph.D. degrees in physics from the Technical University of Kaiserslautern, Germany, in 2004 and 2007, respectively. He has been a Postdoctoral Researcher at the Niels Bohr Institute in Copenhagen, Denmark and at the Max Planck Institute for Dynamics and Self-Organization in Göttingen, Germany and a Guest Lecturer at the Kigali Institute for Science and Technology in Rwanda. Since 2014, he has been heading a Research Group at Forschungszentrum Jülich, Germany.